중력하중 설계된 1:5 축소 3층 철근콘크리트 골조의 지진모의실험

Earthquake Simulation Tests of A 1:5 Scale Gravity Load Designed 3-Story Reinforced Concrete Frame

이한선* 우성우**

Lee, Han Seon Woo, Sung Woo

ABSTRACT

The objective of the research stated herein is to observe the actual responses of a low-rise nonseismic moment-resisting reinforced concrete frame subjected to varied levels of earthquake ground motions. First, the reduction scale for the model was determined as 1:5 considering the capacity of the shaking table to be used and the model was manufactured according to the similitude law. This model was, then, subjected to the shaking table motions simulating Taft N21E component earthquake ground motions, whose peak ground accelerations (PGAs) were modified to 0.12g, 0.2g, 0.3g, and 0.4g. The lateral accelerations and displacements at each story and local deformations at the critical regions of the structure were measured. The base shear was measured by using self-made load cells. Before and after each earthquake simulation test, free vibration tests were performed to find the change in the natural period and damping ratio of the model. The test data on the global and local behaviors are interpreted. The model showed the linear elastic behavior under the Taft N21E motion with the PGA of 0.12g, which represents the design earthquake in Korea. The maximum base shear was 1.8tf, approximately 4.7 times the design base shear. The model revealed fairly good resistance to the higher levels of earthquake simulation tests. The main components of its resistance to the high level of earthquakes appeared to be 1) the high overstrength, 2) the elongation of the fundamental period, and 3) the minor energy dissipation by inelastic deformations. The drifts of the model under these tests were approximately within the allowable limit.

Keywords : Shaking table, Reinforced concrete frame, Earthquake simulation test, Inter-story drift, Base shear, Inelastic behavior, Ductility, Natural period, Damping

* 정회원, 고려대학교 건축공학과 부교수

** 정회원, 고려대학교 건축공학과 박사과정

• 본 논문에 대한 토의를 1999년 4월 30일까지 학회로 보내주시면 1999년 6월호에 토의회답을 게재하겠습니다.

1. Introduction

Recently, minor earthquakes have occurred over 20 times a year in Korea. Particularly the earthquake of December 13, 1996 at Yongwol in Korea imposed significant nonstructural damages. These earthquakes indicate that the Korea Peninsular is no longer safe from the seismic hazard. If a severe earthquake such as the 1995 Kobe earthquake occurred in Seoul, the damage would be tremendous.

Most building structures which are normally medium- to low-rise reinforced concrete frames in Korea have not been engineered to resist major or moderate earthquakes. Therefore, if any major earthquake occurred, the damage or collapse of not only the general commercial buildings, but also public-service buildings such as police offices, communication centers and hospitals would implement very large life and economic losses as well as cause the critical interference with the nation's function.[1]

The objectives of this research are: 1) to observe the actual response of this kind of low-rise nonseismic moment-resisting reinforced concrete frames subjected to varied levels of earthquake ground motions, and 2) to provide the calibration to or to check the reliability of nonlinear time history analyses. However, only the first objective will be dealt with in this paper.

First, the reduction scale for the model was determined as 1:5 considering the capacity of the shaking table. The techniques for manufacturing the model according to the similitude requirements were developed. Using these techniques, a 1:5 scale 2-bay 3-story reinforced concrete frame model was manufactured. This model was, then, subjected to the shaking table motions simulating Taft N21E component earthquake ground motions, whose peak ground acceleration(PGA) was modified to approximately 0.12g, 0.2g, 0.3g, and 0.4g. Before and after each earthquake simulation test, free vibration tests were performed to find the change in the natural period and damping ratio of the model. The global behavior and damage pattern were observed. The lateral accelerations and displacements at each story and the local deformations at the critical regions of the structure were measured. The base shear was measured by using self-made load cells. Based on all the results of these tests, some comparisons and interpretation on the response of the model will be carried out in this paper.

2. Design and Manufacture of Model[2]

2.1 Design of Model

The prototype of this test model was adopted from a building structure for the police office. The plan and elevation of the 1:5 scale model are shown in Fig. 1(a) and (b). The compressive strength of concrete f_c' is assumed 210 kgf/cm^2 and the nominal yield strength of reinforcement 3,000 kgf/cm^2. The typical sections of members and the details regarding transverse steel, anchorage and splice are shown in Fig. 1(c) to (g).

The important characteristics in these nonseismic details are:

1) the splice is located at the bottom of the column,

2) the spacing of hoops is large,

3) no use of seismic hooks,

4) no hoops in beam-column joints, and

5) the anchorage of reinforcement in the joints.

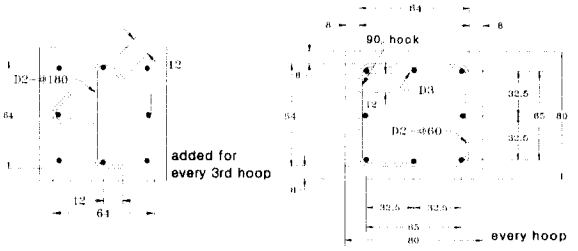

(c) Column (C2*) : * See (d) and (f) for C2

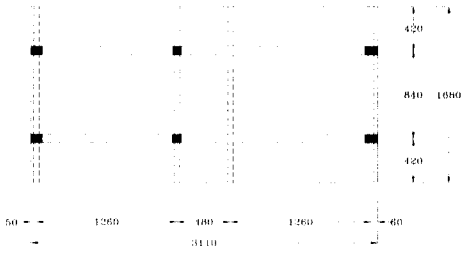

(a) Plan

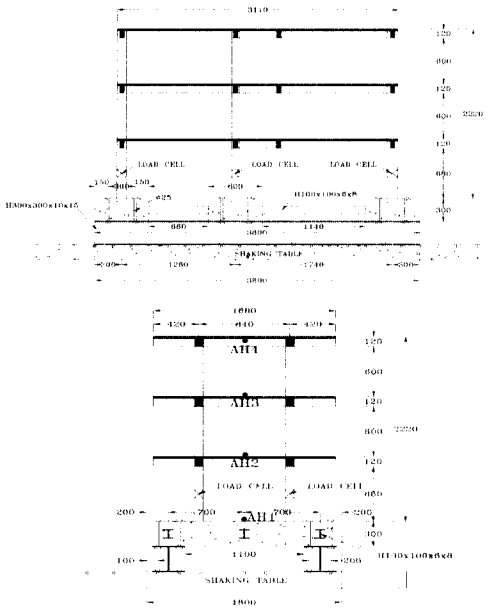

(b) Elevation

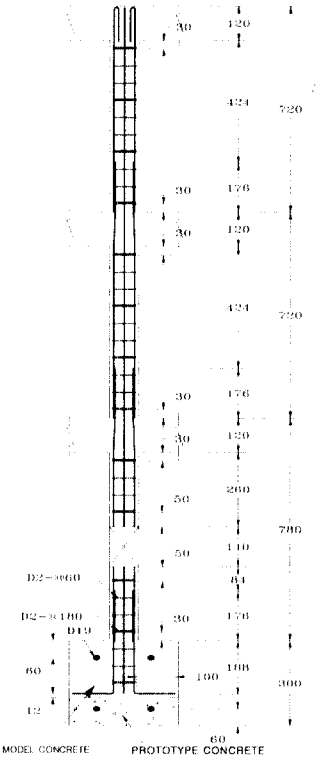

(d) Transverse steel for column (C2*)

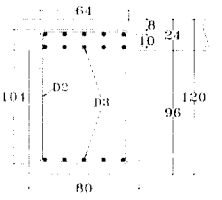

(e) Beam (Section A-A' in (f))

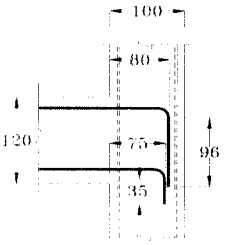

(g) Detail for an external beam-column joint

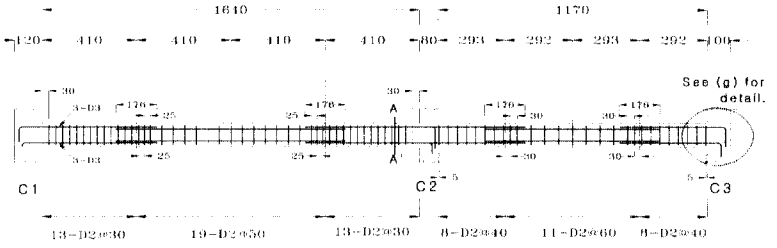

(f) Transverse steel for beams

Fig. 1 Plan, elevation and details (unit : mm)

2.2 Manufacture of Model

Model Reinforcement

It is essential to maintain the similitude in the material properties between prototype and model reinforcement. However, it was found difficult to make the cross sections of the model reinforcement conform exactly to the similitude law. So, the yielding forces rather than yielding stresses were selected as the target to be achieved in annealing the model reinforcement. A 3-zone vacuum tube electric furnace as shown in Fig. 2 was designed and used. The deformation on the surface of the model reinforcements was made using a deforming device. D22 and D10 bars in full-scale structure match D3 and D2 in the model, respectively. The typical load-strain relations for D3 and D2 are shown schematically in Fig. 3. The target yielding forces derived from similitude requirements are shown in Table 1.

Model Concrete

Model concrete was made using type I portland cement and the mix ratio is shown in Table 2 with the definition of fine and coarse aggregates given in the footnotes. The average strength of model concrete at the time of test is about 220 kgf/cm^2.

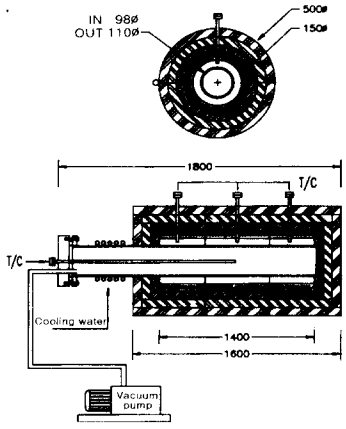

Fig. 2 3-zone vacuum tube electric furnace (unit :mm)

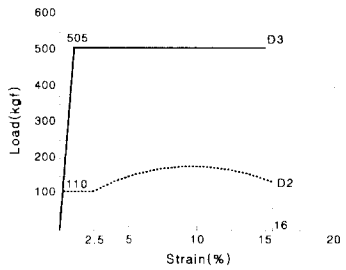

Fig. 3 Average load-strain relations of model reinforcements

2.3 Experimental Setup and Instrumentation

2.3.1 Shaking Table

The used shaking table located in Hyundai Institute of Construction

Table 1 Similitude requirements for reinforcements

Member and Use		Prototype (stress)			1/5 Model (force)		
Beam	Column	Bar	Yield Strength kgf/cm^2	Tensile Strength kgf/cm^2	Bar	Yield Strength kgf	Tensile Strength kgf
Stirrup	Hoop	D10	3,650	5,413	D1.9	104.1	154.4
Main Reinforcement		D22	3,650	5,413	D3	565.2	838.1

Table 2 Mix ratio of concrete

W/C(%)	Water	Cement	Sand*	Gravel**	Super-plasticizer
60	212.4kg	353.4kg	674.3kg	353.4kg	2.5g

* Sand is defined as river sand particles passing 2.5mm sieve.

** Gravel is defined as crushed rock particles passing 5.0mm sieve but remaining in 2.5mm sieve.

Technology has the size of 3m×5m and 1 degree-of-freedom. The capacity of this shaking table can be presented by the plot given in Fig. 4.

The input Taft N21E(PGA = 0.12g) motion and the output table motion are compared in Fig. 5. From this figure, it can be found that the fidelity of shaking table is satisfactory.

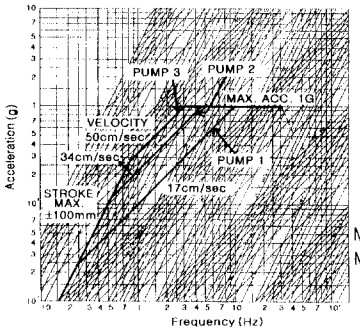

Capacity : + 40 ton
Max. Stroke : + 100 mm
Max. Velocity : 50 cm/sec
Max. Acceleration : 1 g
Max. Load : 30 ton

Fig. 4 Shaking table system

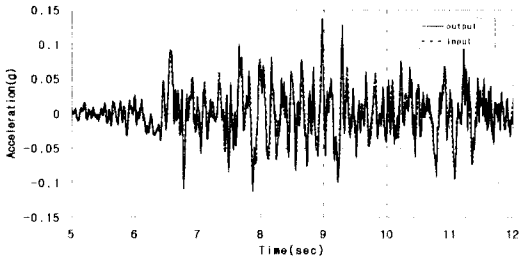

Fig. 5 Output shaking table motion for input Taft N21E 0.12g

2.3.2 Data Acquisition System and Instrumentation

The flow of the control and data acquisition system is shown in Fig. 6. The data can be acquired simultaneously at the rate of 300Hz up to 32 channels.

Displacement transducers, accelerometers and load cells were used to measure the lateral displacement and acceleration at each story, shear forces at the columns of the first story, and the rotational angles in some ends of beams and columns.

Fig. 7 shows the instrumentation to the model and Table 3 gives the number of each type of transducers. To measure story drifts, a reference frame was used as shown in Fig. 7. The load cells were designed and made following Bertero et al.[3] and calibrated by using Universal Testing Machine.

Table 3 Type and number of sensors (unit : ea)

	Displacement transducer (for story drift)	Accelero -meter	Load cell	Displacement transducer (for local rotations)
Table	1(D1)	1(AH1)	3	
Second Floor	1(D2)	1(AH2)		6 (for beam)
Third Floor	1(D3)	1(AH3)		12 (for column)
Roof	2(D4, D5)	1(AH4)		
Subtotal	5	4	3	18
Total : 30				

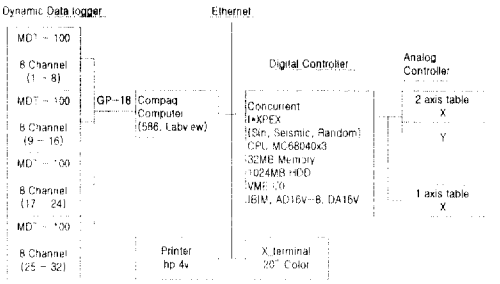

Fig. 6 Flow of control and data acquisition system

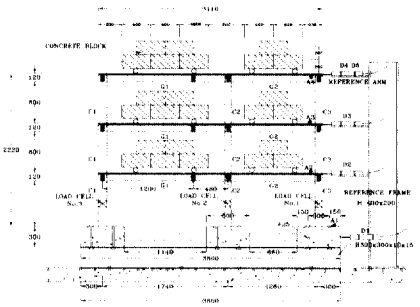

Fig. 7 Instrumentation (unit : mm)

2.3.3 Artificial Mass

The volume of the model is reduced to $1/5^3$ of the prototype while the similitude law premising the agreement in the

stress-strain relation requires the mass reduced to $1/5^2$. Therefore, the compensation for the difference should be artificially made by adding concrete blocks shown in Fig. 7. The total weight of the model with concrete blocks is about 10.3tf. The hinges between the model and the concrete blocks as shown in Fig. 7 were designed to transmit only the vertical and horizontal forces except the moments due to the mass of the concrete block. Photo 1 shows the overall view to the experimental setup and instrumentations for the model.

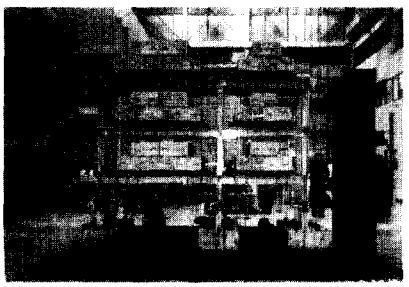

Photo. 1 Experimental setup

2.4 Test Program

The program of tests is shown in Table 4. Before and after each earthquake simulation test, free vibration tests were performed to check the natural period and damping ratio. The adopted input ground accelerogram is the Taft N21E component. But the peak ground acceleration (PGA) was modified to 0.12g, 0.2g, 0.3g, and 0.4g. Each inputmotion represents the earthquake stated in the remarks of the table.

3. Test Results and Interpretation[4), 5)]

3.1 Natural Period and Damping Ratio

Free vibration tests were performed by enforcing and releasing the initial lateral displacement of approximately 1~2mm at the roof of the model.

From these tests, the natural periods and damping ratios of the model were obtained by using the Fourier transform and logarithmic decrement method. Fig. 8(a) and (b) show that natural period and damping ratio tend to increase as the model experiences higher levels of ground motions.

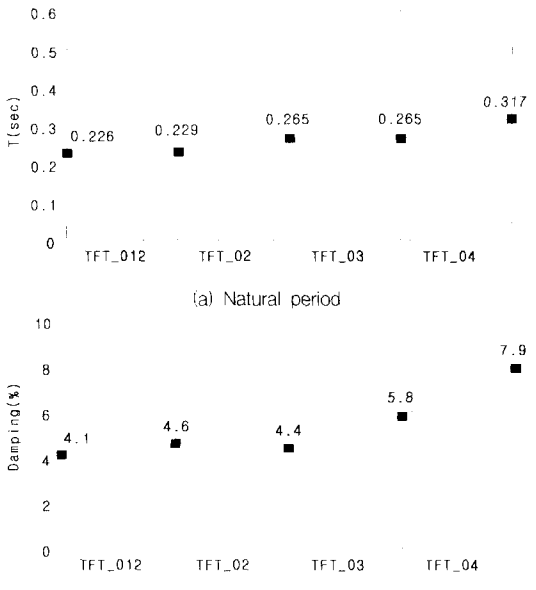

Fig. 8 Natural period and damping ratio

3.2 Global Responses

Table 4 Test program

Identification of Test	Type(PGA)	Remarks (Return Period)
TFT 012	Taft N21E(0.12g)	Design earthquake in Korea(475 years)
TFT 02	Taft N21E(0.2g)	Max. earthquake in Korea(1,000 years)
TFT 03	Taft N21E(0.3g)	Max. considered earthquake in Korea (2,000 years)
TFT 04	Taft N21E(0.4g)	Severe earthquake in high seismic regions of the world

3.2.1 Floor Accelerations

The drifts at the roof were measured at two locations as shown in Table 3. The test results shown in Fig. 9 indicate that there occurred almost negligible torsional behavior in this model. Therefore, from here on, the measured data in one of the two plane frames are assumed to represent the behavior of both frames.

Table 5 shows the accelerations at each floor at the time when the roof undergoes the maximum acceleration. Also, the dynamic amplification factors, $\ddot{a}_{roof\max} / \ddot{a}_{table\max}$, are shown in this table. This amplification factor tends to decrease due to the energy dissipation by inelastic deformations as the model became subjected to higher levels of table motions.

Time histories of the floor accelerations for the shaking table motion simulating Taft N21E 0.2g are given in Fig. 10. The response has the predominant period approximately equal to the period of the first mode of the model.

3.2.2 Story Drift and Inter-story Drift Indices

Table 6 shows the drifts at each floor

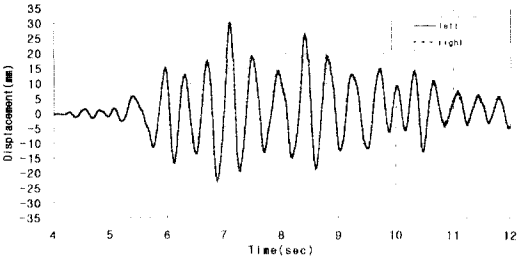

Fig. 9 Time histories of drifts at roof (TFT_04)

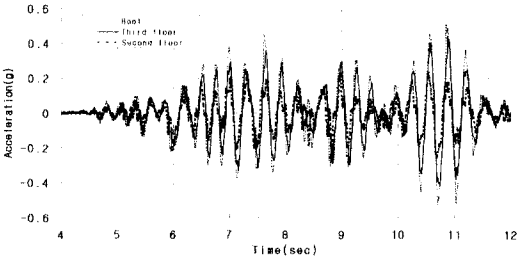

Fig. 10 Time histories of floor accelerations for TFT_02

at the time when the roof undergoes the maximum. The inter-story drift indices(I.D.I.) are also given. For the design earthquake of Korea (TFT_012), the model has the maximum I.D.I., 0.26%, which is less than the maximum allowable value, 1.5%/4.5 = 0.33%. The maximum I.D.I. for Taft N21E 0.4g table motion appears 1.68%, which is a little larger than the maximum allowable, 1.5%. Therefore, regarding the drift control, the behavior of the model turns

Table 5 Maximum horizontal accelerations

Test	Max. acceleration(g)				Dynamic amplification factor ($\ddot{a}_{roof\max} / \ddot{a}_{table\max}$)
	Table	Second floor	Third floor	Roof	
TFT_012	0.138	0.13	0.23	0.28	2.03
TFT_02	0.21	0.22	0.37	0.53	2.52
TFT_03	0.31	0.13	0.49	0.61	1.97
TFT_04	0.4	0.22	0.51	0.69	1.73

Table 6 Maximum inter-story drifts

Test	Max. drifts(mm)			Inter-story drift index(%)		
	Second floor	Third floor	Roof	First story	Second story	Third story
TFT_012	2.02	3.69	4.5	0.26	0.23	0.11
TFT_02	6.06	11.36	14.06	0.77	0.74	0.38
TFT_03	7.25	14.99	17.87	0.93	1.08	0.4
TFT_04	12.28	24.40	29.88	1.57	1.68	0.76

out to be satisfactory.

The time histories of story drifts are shown in Fig. 12 for Taft N21E 0.2g table motion. From this figure, the predominance of the first mode can be observed.

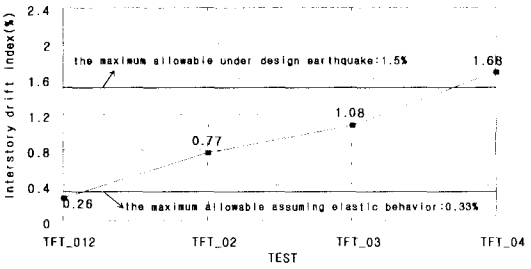

Fig. 11 Inter-story drift index

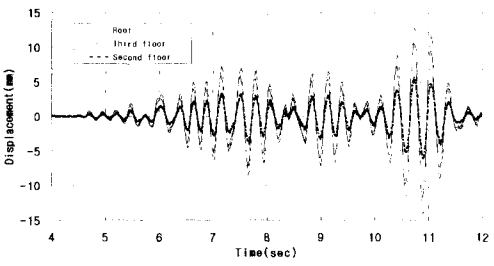

Fig. 12 Time histories of story drifts for TFT_02

3.2.3 Base Shear versus Inter-story Drift at First Story

Fig. 13 shows the hysteretic relation between the measured base shear and the inter-story drift at the first story. The model behaves linear elastically under the table motion simulating Taft N21E 0.12g, which represents the design earthquake in Korea. The developed maximum base shear was 1.8tf. The maximum base shears for other table motions are given in Table 7. It can be clearly noted that the model has yielded under the shaking table motion simulating Taft N21E 0.4g. Here the yielding base shear appears 3.79tf.

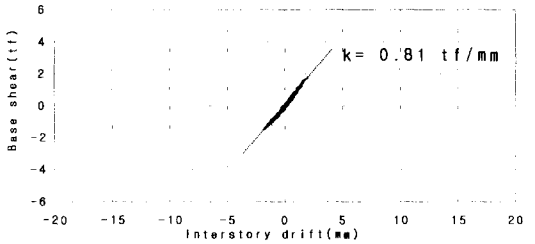

(a) TFT_012

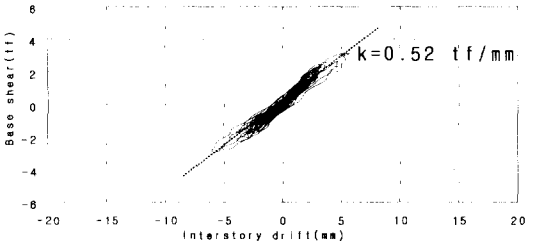

(b) TFT_02

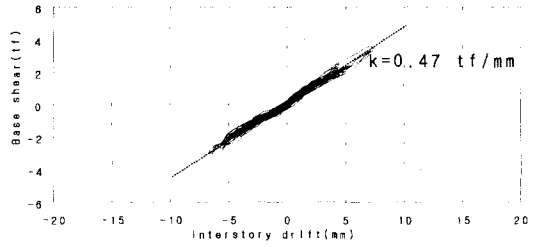

(c) TFT_03

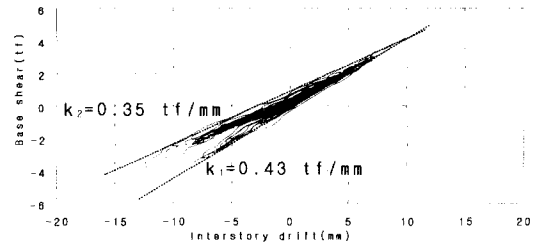

(d) TFT_04

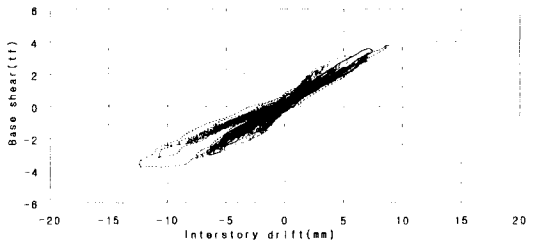

(e) superposition

Fig. 13 Relation between base shear and inter-story drift at first story

Table 7 Maximum base shears and average stiffnesses at first story

Test	Max. base shear(tf)	Story stiffness at first story(tf/mm)
TFT 012	1.8	0.81
TFT 02	3.14	0.52
TFT 03	3.58	0.47
TFT 04	3.79	0.35~0.43

3.2.4 Ratio of Base Shear to Weight

For reference, the seismic coefficient for the moment-resisting reinforced concrete frame is calculated as follows.

$$C_s\left(=\frac{V}{W}\right)=\frac{AISC}{R}=\frac{(0.12)(1.0)(1.39)}{4.5}$$
$$=0.037$$

Where, V : base shear
W : effective weight of the structure
A : 0.12 (zone factor)
I : 1.0 (importance factor)
T : $0.23\times\sqrt{5}$(scale factor)
= 0.514sec (natural period)
C : $\frac{1}{1.2\sqrt{T}}=1.162\leq 1.5$ (dynamic factor)
S : 1.2 (soil factor)
SC : 1.39 (but should be less than 1.75.)
R : 4.5 (response modification factor)

Fig. 14 shows the ratio of the measured maximum base shear to the weight of the model. For the table motion (Taft N21E 0.12g) simulating the design earthquake in Korea, the actually developed maximum base shear is about 4.7 times the design base shear.

It can be noted from Fig. 14 that this model resisted the table motions of higher PGA's with very high lateral strength up to approximately 0.37W. Also the degradation of stiffness has elongated the natural period of the model and hence caused the decreased dynamic amplification factor. For the table motions simulating Taft N21E 0.4g earthquake, the model has yielded and shown that the global displacement ductility is about 1.23. Considering these phenomena, it can be concluded that the model behaves linear elastically under the design earthquake (PGA ≅ 0.12g) while for the higher table motions (PGA = 0.2g, 0.3g, and 0.4g), the overstrength up to 0.37W, the degradation of stiffness and the energy dissipation due to inelastic behavior in the model were the additional major contributors to its resistance.

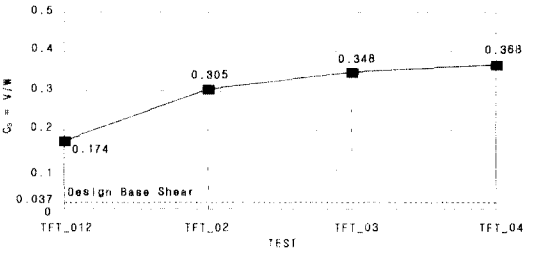

Fig. 14 Ratio of max. base shear to weight of model

3.3 Local Responses

The angular rotations in the ends of beams and columns are measured as shown in Fig. 15. The distance to measure this rotational angle is effective depth d for beams and the cross-sectional dimension h parallel to the shaking direction for columns.

The maximum angular rotations are shown in Table 8 for each earthquake simulation test. The bottom end of the interior column at the second story has shown the largest rotational angle of all the measured locations. Relatively large rotations occurred for the interior columns. For the exterior joint, the beam has larger rotation than the columns. Noting that the model has smaller cross-section in the interior column than in the exterior columns, this larger rotation in the interior column can be expected.

As shown in Fig. 16(a) and (b), the rotational angles at the beams are much less than those at columns in the case of the interior joint. On the contrary, the rotation at the beam is larger than those at the columns in the case of the exterior joint as given in Fig. 17. Also, the permanent rotational deformation can be noticed in the end of the beam in this figure.

Table 8 Maximum angular rotation (unit : 10^{-4}rad)

Test \ Location	1	2	3	4	5	6	7	8	9
TFT_012	17	23	10	27	10	12	11	20	6
TFT_02	60	68	22	100	33	40	34	70	21
TFT_03	66	96	55	130	50	57	44	90	31
TFT_04	134	154	85	241	76	75	50	141	42

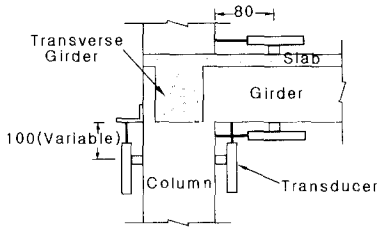

Fig. 15 Dimension and location of transducers to measure angular rotations (unit : mm)

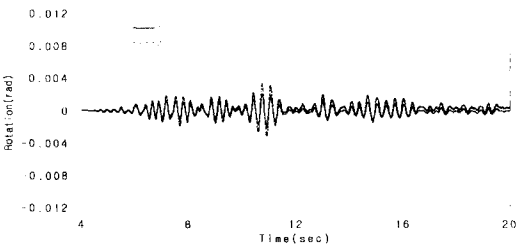

(a) Beam ends

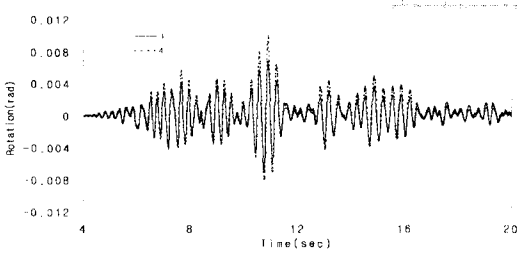

(b) Column ends

Fig. 16 Angular rotations at interior joint under TFT_02

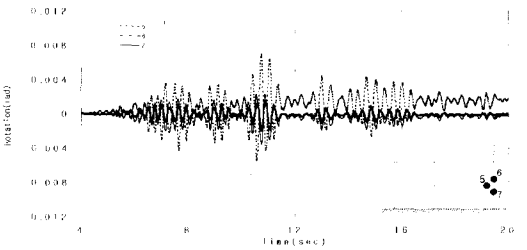

Fig. 17 Angular rotations at exterior joint under TFT_02

The Fig. 18 shows the distribution of shear forces for the columns. It is interesting to note that column 1 and column 3 have unilateral shear forces due to the influence of the axial compressive force on the shear resistance.

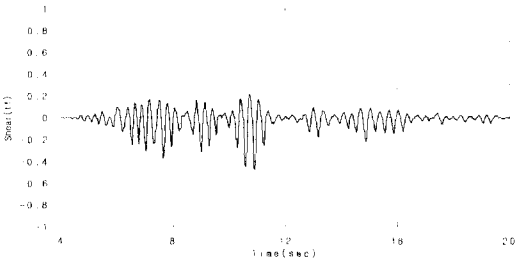

(a) column 1

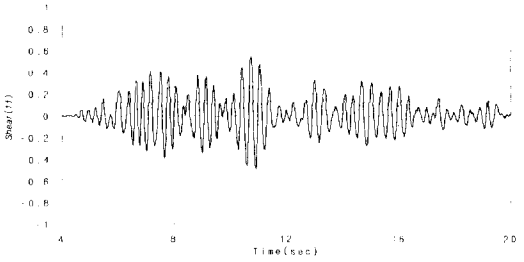

(b) column 2

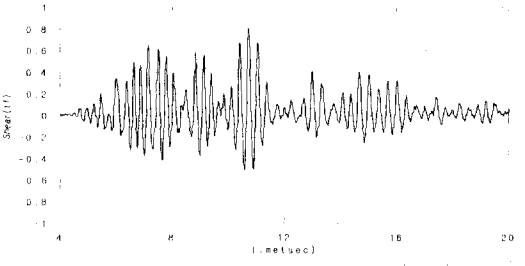

(c) column 3

Fig. 18 Column shears under TFT_02

3.4 Crack Pattern

The model did not show serious damage even after the test of Taft N21E 0.4g simulating the severe earthquake in the high seismic zone of the world. There was no apparent crack after Taft N21E 0.12g and Taft N21E 0.2g tests. After Taft N21E 0.3g test the flexural crack can be noticed at the location (1) in Fig. 19. Several cracks occurred for the test of Taft N21E 0.4g as shown in Fig. 19.

The beam ends at the exterior joint of the second floor have significant cracks at locations (2), (3), (4), (5), in Fig. 19, and this implies the yield. In particular, the exterior columns at the first story have revealed both the flexural and shear cracks at locations (6), (7) and (8) as shown in this figure. However, it is interesting to note that the interior columns, which have experienced larger rotations, did not show any apparent cracks. The photos 2 and 3 show the detail of cracks at locations shown in Fig. 19.

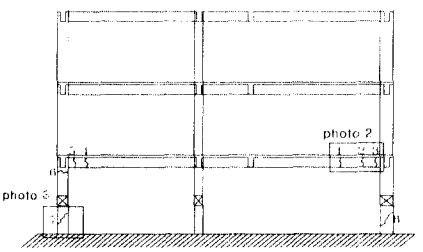

Fig. 19 Crack pattern

4. Conclusions

(1) The fact that the behavior of the model subjected to the shaking table motion representing the design earthquake was entirely linear elastic and that the maximum base shear, 1.8tf, was

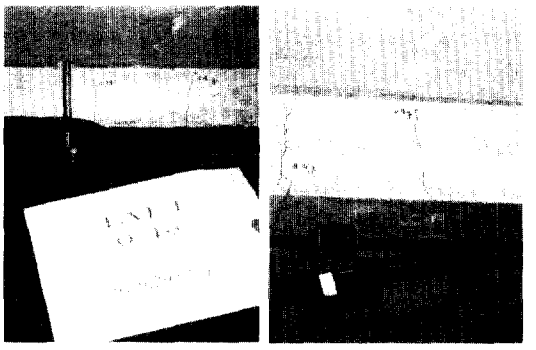

Photo. 2 cracks at the second-floor beam

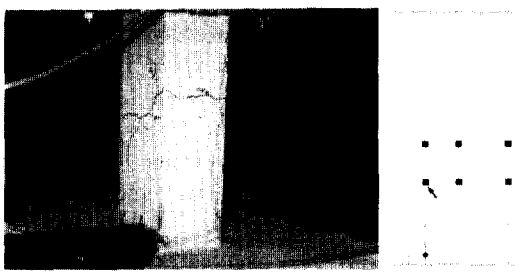

Photo. 3 cracks at the first-story column

4.7 times the design base shear of the Korean code implies that the concept of ductility in the response and therefore in the design of low-rise reinforced concrete structures may be inappropriate to apply in the moderate or low-intensity seismic zones such as in Korea.

(2) The prominent components of resistance in the moment-resisting low-rise reinforced concrete frame to the higher level of shaking table motions are the very large overstrength, the degradation of stiffness (i.e. elongations of the first-mode period), and the relatively minor energy dissipation by inelastic deformations.

(3) Though the model represents nonseismic gravity-load-designed moment -resisting reinforced concrete structures, its earthquake-resistant capacity turns

out excellent. However, it may not be appropriate to derive a general conclusion on the seismic performance of low-rise nonseismic reinforced concrete frames just with these limited test results.

Acknowledgements

The research stated herein was supported by the Ministry of Construction and Transportation, the Republic of Korea, and several private companies including SSangYong Engineering and Construction Corp., DongBu Corp., Hyundai Construction Corp., and DongYang Structural Safety Consultants Corp. These supports are acknowledged gratefully by the writers. The contributions of Dr. Ha-Seon Jeong and Dr. Jin-Kyu Song at Hyundai Institute of Construction Technology, and graduate students at Korea University, Dong-Woo Ko, Yun-Sup Heo and Kyi-Yong Kang, were critical to the success of this research and are also appreciated.

References

1. Kim, S.-D., Lee, H.-S., Kim, Y.-M., and others, "A Study on the Seismic Evaluation and Retrofit of Low-rise Reinforced Concrete Building in Korea," Ministry of Construction and Transportation, Republic of Korea, R&D 96-0057, December 1997, 804pp.
2. Lee, H.-S., Woo, S.-W., and others, "Manufacturing Technique and Material Properties for 1/5-Scale Reinforced Concrete Frame Model," Proceeding of Autumn Conference in 1997, Korea Concrete Institute, Vol. 9, No. 2, November 1997, pp 575-580.
3. V. V. Bertero, A. E. Aktan, A. A. Chowdhury, T. Nagashima, "Experimental and Analytical Characteristics of A 1/5-Scale model of A 7-Story R/C Frame-Wall Building Structure," Earthquake Engineering Research Center, Report No. UCB/EERC-83/13, August 1983, pp 83-84.
4. Lee, H.-S., Woo, S.-W., and others, "Shaking Table Tests of A 1/5-Scale 3-Story Nonductile Reinforced Concrete Frame," Proceeding of Autumn Conference in 1997, Korea Concrete Institute, Vol. 9, No. 2, November 1997, pp 581-586.
5. Lee, H.-S., Woo, S.-W., and Heo, Y.-S., "Inelastic Behaviors of A 3-Story Reinforced Concrete Frame with Nonseismic Details," Proceeding of Spring Conference in 1998, Korea Concrete Institute, Vol. 10, No. 1, May 1998, pp 427-432.

요 약

이 연구의 목적은 여러 수준의 지진에 대한 비내진 상세를 가진 저층 모멘트 저항 골조의 실제 반응을 관찰하기 위한 것이다. 우선, 모델에 대한 축소율은 사용된 진동대의 용량을 고려하여 1:5로 결정하였으며 상사성의 법칙에 따라 모델을 제작하였다. 그 다음에 이 모델에 대해 Taft N21E 지진가속도 기록의 최대 지진가속도를 0.12g, 0.2g, 0.3g, 0.4g로 조정하여 진동대를 이용한 지진모의실험을 수행하였다. 각 층별 횡방향 가속도와 변위, 그리고 구조물의 취약부위에서 국부변형이 측정되었다. 밑면 전단력은 손수 만든 로드셀을 이용하여 측정하였다. 각 지진모의실험 전과 후에는 고유주기와 감쇠비의 변화를 살펴보기 위해 자유진동실험을 수행하였다. 전체거동과 국부거동에 대한 실험결과를 분석한 결과, 이 모델은 우리나라의 현행 내진 설계 기준에서의 설계지진 즉, 0.12g의 최대 지진가속도에 대해서는 선형탄성으로 거동하였다. 최대 밑면 전단력은 1.8tf로 설계 밑면 전단력의 약 4.7배로 나타났다. 이 실험모델은 높은 수준의 지진모의실험에서도 양호한 성능을 나타내었다. 높은 수준의 지진에 대한 저항의 주요소는 1) 높은 초과강도, 2) 기본주기의 증가, 그리고 3) 비탄성 변형에 의한 얼마간의 에너지 소산이다. 이 실험에서 모델의 층간변위는 대략 허용한계 내에 있었다.

(접수일자 1998. 7. 28)